HYDRIDE DEVELOPMENT FOR HYDROGEN STORAGE

K. J. Gross, E. Majzoub, G.J. Thomas, and G. Sandrock
Sandia National Laboratories
Livermore, CA 94550

Abstract

Ti-doped Alanates offer an entirely new prospect for lightweight hydrogen storage. These materials have nearly ideal equilibrium thermodynamics, good packing densities, moderate volume expansion and useful sintering properties. However, there is much room for improving both absorption and desorption kinetics, and the less-than-theoretical reversible capacities. Our work has focused on finding solutions to these problems to achieve the performance requirements needed to supply onboard hydrogen for PEM fuel cell powered vehicles.

Two new generations of materials have been developed. These are; Generation III and Generation IV Ti-doped sodium alanates that are synthesized directly from NaH, Al, Ti-dopant and Na-metal, Al, Ti-dopant respectively. These materials have demonstrated better kinetics than materials produced using earlier methods. In addition, the direct synthesis is performed without the use of solvents. The result is a hydrogen storage material that is less-expensive to produce and delivers hydrogen free of hydrocarbon impurities.

To improve capacity we have investigated the use of Ti-halides other than $TiCl_3$ to catalyze hydrogen absorption and desorption in $NaAlH_4$. TiF_3 and $TiCl_2$ appear to work equally as well as $TiCl_3$ and reduce the overall capacity loss due to the formation of NaCl or NaF.

Scaled-up engineering properties studies and cycle-life measurements are also performed. Initial results from some of those measurements will also be presented.

Introduction

The alkali metal alanates are compounds belonging to the larger class of complex hydrides. In the past, they were known to liberate copious amounts of hydrogen either by direct thermal decomposition or by one-time hydrolysis. However, they were generally considered irreversible and, therefore, not useful for practical hydrogen storage applications. This was until Bogdanovic et al (Bogdanovic' 1997) demonstrated that the alanate, $NaAlH_4$, would reversible desorb and absorbed hydrogen under relatively mild conditions when doped with Ti-based catalyst. Since that time there has been a growing body of work in characterizing catalyzed alanates, as well as the development of new catalysts and methods of preparation (Bogdanovic' 2000, 2001, Jensen 1999, 2001, Zidan 1999, Zaluska 2000, 2001, Gross 1999, Thomas 1999).

Unlike the interstitial intermetallic hydrides, the alanates release hydrogen through a series of decomposition / recombination reactions:

$$NaAlH_4 \Leftrightarrow 1/3Na_3AlH_6 + 2/3Al + H_2 \Leftrightarrow NaH + Al + 3/2H_2 \quad \text{(Eq.1)}$$

The two combined reactions give a theoretical reversible hydrogen storage capacity of 5.6 wt.%. Previous studies showed that the first reaction will release 1 atm of H_2 at 33°C and the second reaction releases 1 atm of H_2 at 126°C (Bogdanovic' 2000, Gross 2000). This is shown in the v'ant Hoff diagram of Figure 1.

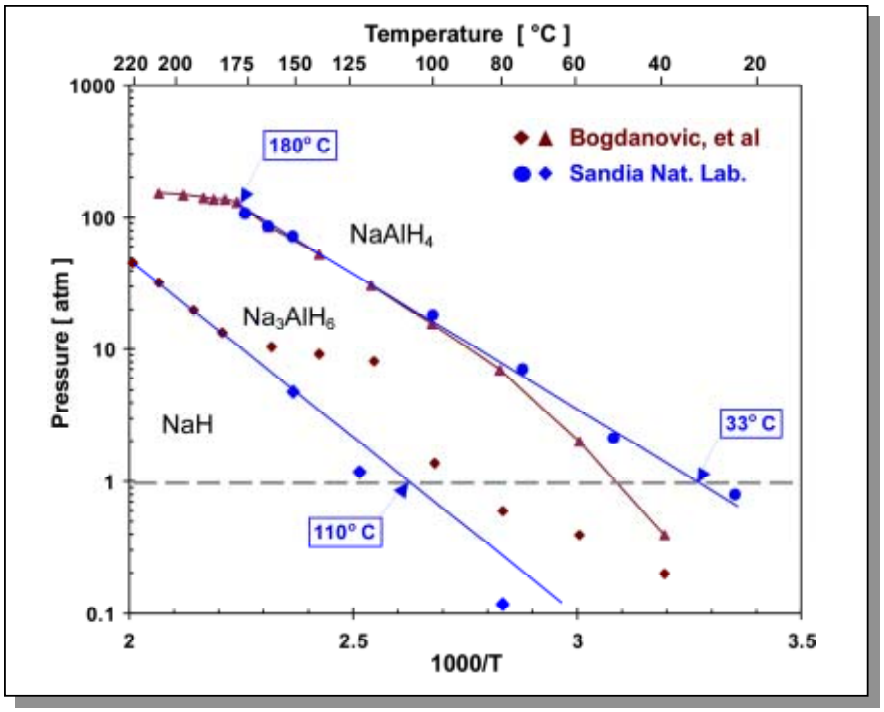

Figure 1 – Van't Hoff Diagram showing equilibrium pressures as a function of temperature for both alanate phases

Experimental Basics

Generation II materials: Crystalline $NaAlH_4$ was made by cryopumping THF from a 1.0M solution of $NaAlH_4$ in THF (Aldrich Chemical No. 40,424-1), followed by vacuum drying with a mechanical and/or turbomolecular pump. Mixtures of $NaAlH_4$ and solid $TiCl_3$ (99.999% Aldrich Chemical No. 51,438-1) were weighed in a purified argon glovebox in the levels of 0.9, 2, 4, 6 and 9 mol% $TiCl_3$. These mixtures were then ball-milled in argon for 3 hours, using a high-energy SPEX® mill and WC balls and milling vial. The powder to ball weight ratio was approximately 10:1. Samples were transferred from the milling pot to the reactor vessel in the Ar glovebox. X-ray diffraction, using airless sample holders, was done before and after milling; in all cases the conversion of $TiCl_3$ to NaCl (Eq.2) during milling was confirmed.

Generation III and IV materials: (Patent application submitted) Aluminum powder (~20 micron, 99+% Aldrich Chemical No. 26,651-5), NaH 95% Aldrich Chemical No. 22,344-1), and solid $TiCl_3$ (99.999% Aldrich Chemical No. 51,438-1) were weighed into appropriate proportions in a purified argon glovebox. These were then mixed and sealed under argon into a tungsten-carbide milling vial. These mixtures were then ball-milled in argon for 2 hours, using a high-energy SPEX® mill. The powder to ball weight ratio was approximately 10:1. After milling, about 1.5 grams of the mixture was transferred (again under an argon atmosphere) to a stainless steel reactor vessel with an internal volume of about 16 cm^3 and exposed to high purity (Matheson Trigas research purity 99.999 %) hydrogen gas pressurized to between about 80 atm to about 100 atm while the steel reactor and its contents are heated externally to about 125°C for up to 20 hours.

Dehydriding and hydriding rates and capacities were obtained volumetrically using a Sieverts' apparatus and a cylindrical 316 SS reactor (1.3 cm outer diameter by 0.12 cm wall thickness and length of 12cm) containing about 1.5 g of catalyzed samples. A thermocouple well in the center of the vessel allows for accurate temperature measurements during cycling. Absorption pressure changes were quantified with a calibrated 200 atma pressure transducer and desorption pressures with a 1000 Torr (1.3 atma) Baratron® capacitance manometer. Data were recorded via computer and measurements lasted from minutes to several days, depending on the $TiCl_3$, level test pressure, and temperature conditions.

During absorption, the applied H_2 pressure was generally in the 80-90 atm range, well above the 30-40 atm plateau pressure for $NaAlH_4$ at 125˚C. For the desorption experiments, the back-pressure during $NaAlH_4$ decomposition was kept below 1 atma and during Na_3AlH_6 decomposition below 0.25 atma, well below the Na_3AlH_6 plateau pressure of about 2 atma. Hydrogen capacity data are presented as weight % with respect to the total sample weight, including the catalyst.

Isothermal Arrhenius analyses was performed as follows. Measurements were started after several hydriding/dehydriding cycles with samples in the fully hydrided condition and cooled to room temperature. The pressure rise from desorption into a known volume at a given temperature was measured, the temperature was then increased. The desorption rates were determined at each temperature from the slope of the essentially linear increase in pressure with time. This procedure was continued up to 150˚C. The sample was held at this temperature until the $NaAlH_4$ decomposition step (Eq.1) was finished. The sample was then quickly cooled and the Na_3AlH_6 rates determined by the same procedure. The rate data are presented as moles of desorbed hydrogen per mole active sodium per hour.

Experimental Results – Generation II Alanates

Our initial studies focused on what we now refer to as Generation II materials (Gross 2000, 2001a, Sandrock 2001). These consisted of $NaAlH_4$ dried from THF solution and ball milled with varying levels of solid $TiCl_3$.

Capacity Loss with Increasing Catalyst Content

XRD results showed that $NaAlH_4$ and $TiCl_3$ react during the milling process to form NaCl (Gross 2001b). The same has been found to be true for TiF_3 and $TiCl_2$. The amount of $NaAlH_4$ that is rendered inactive by decomposition into NaCl and Al is proportional to the quantity of added Ti-halide. The total reversible hydrogen capacity decreases as the Ti-halide doping level is increased (Figure 2). A small advantage is gained by using both TiF_3 and $TiCl_2$. At higher doping

levels it is anticipated that $TiCl_2$ will provide a reasonable improvement in capacity, since only two moles of $NaAlH_4$ are lost per mole of $TiCl_2$ versus three moles for $TiCl_3$.

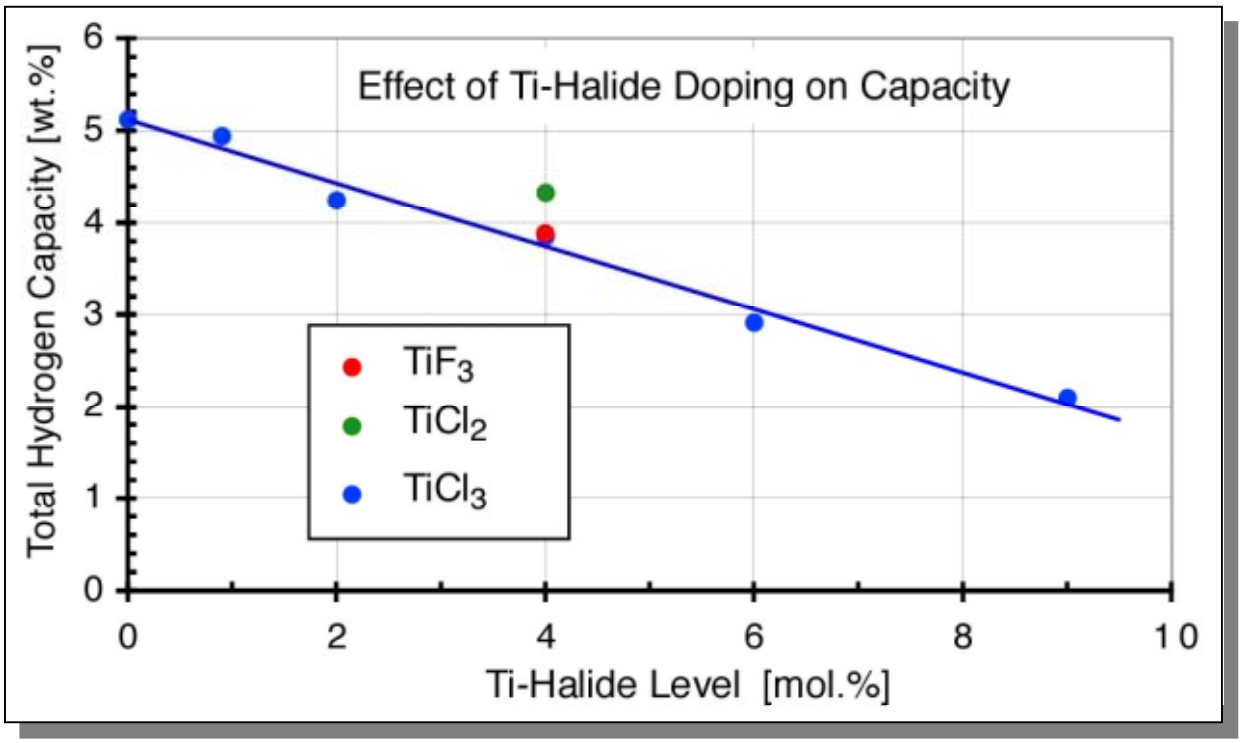

Figure 2 – Reversible hydrogen capacity as a function of $TiCl_3$ content.

Improved Kinetics with Increasing Catalyst Content

Contrary to the generally held view, the rates of hydrogen absorption and desorption are strongly dependent on the level of catalyst doping (Sandrock 2002). It was found that the addition of even a minor amount (1 mol.%) of $TiCl_3$ significantly reduced the activation energy of decomposition for both $NaAlH_4$ and Na_3AlH_6. The addition of more $TiCl_3$ had no further effect on the activation energy. However, the rates of decomposition did continue to increase as the level of $TiCl_3$ was increased. This was due to an increase in the pre-exponential factor ***k*** for the rate equation,

$$Rate = k\ exp(-Q/RT) \qquad \textbf{(Eq.2)}$$

possibly indicating Ti-induced enhanced diffusion of hydrogen and/or metal species.

The desorption rates at 125° for $NaAlH_4$ and Na_3AlH_6 doped with 0.9, 2, 4, 6 and 9 mol% $TiCl_3$ are shown in Figure 3. Figures 2 and 3 make it clear that there is a trade-off between improved kinetic performance and the reversible capacity as the level of Ti-doping is increased. This effect will be critical in selecting the correct material composition for a given hydrogen storage application. Further analysis along these lines is planned, in particular with respect to the rates of reformation (hydrogen loading).

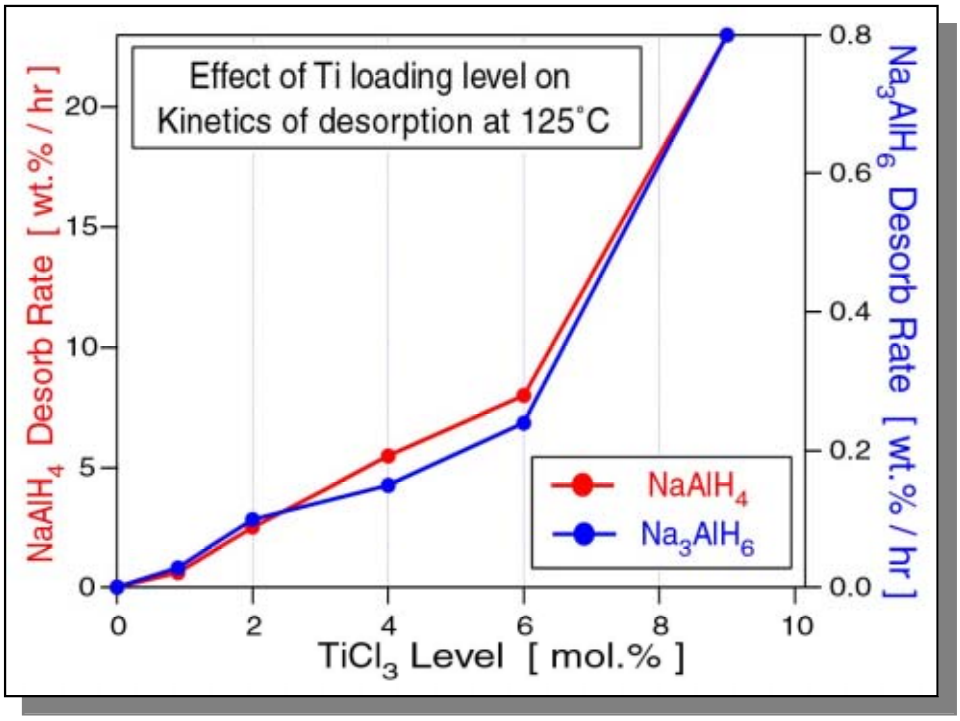

Figure 3 – Rates of hydrogen desorption as a function of $TiCl_3$ content for the decompositions of $NaAlH_4$ and Na_3AlH_6.

Identical Kinetics for Different Ti-Halides

Next we examined the effect on kinetics of using different titanium-halide precursors. Figure 4 shows an Arrhenius plot of the log of the desorption rates of $NaAlH_4$ versus inverse temperature for samples doped with two different Ti-halides ($TiCl_3$ and TiF_3 4 mol.%). Arrhenius plots of the undoped material and 8 mol.% $TiCl_3$ are also shown for comparison. All samples were prepared by the direct synthesis method (Generation III) with the exception of the undoped sample and one of the 4 mol.% $TiCl_3$ samples (Generation II materials labeled "prior art"). These two samples used $NaAlH_4$ precipitated from solution. The kinetic results of the TiF_3–doped samples are nearly identical to those doped with $TiCl_3$. This is true, both in terms of the rates and the activation energy (slope) for the two different halides. The degree to which the results are similar becomes apparent when compared to the effect that different Ti-loading levels has on kinetics. We conclude that enhanced kinetics is solely due to the introduction of Ti and is independent of the type of halide precursor that is used. The activation energy, therefore the mechanism of Ti-enhances kinetics is unchanged by using different Ti-halides.

Cycle-life Measurements

$NaAlH_4$ doped with 4 mol.% $TiCl_3$ cycled up to 116 times continued to show reversible hydrogen absorption. Quantitative cycle-life measurements are now in progress. Figure 5 shows the 34th through 37th desorption half-cycles of a Generation III $NaAlH_4$ sample doped with 4 mol.% $TiCl_3$. In cycle no. 34 the temperature was increased from 125°C to 140°C. This caused the observed increase in the rate of hydrogen desorption. The bend in each of the desorption curves at about

2.5 wt.% H_2 corresponds to completion of the decomposition of $NaAlH_4$. The remaining hydrogen evolution is due to the decomposition of Na_3AlH_6. The rates of hydrogen absorption and desorption increased dramatically in the first three cycles. This indicates an activation process. After these initial cycles, the sample showed very stable reversible hydrogen capacities and sorption rates.

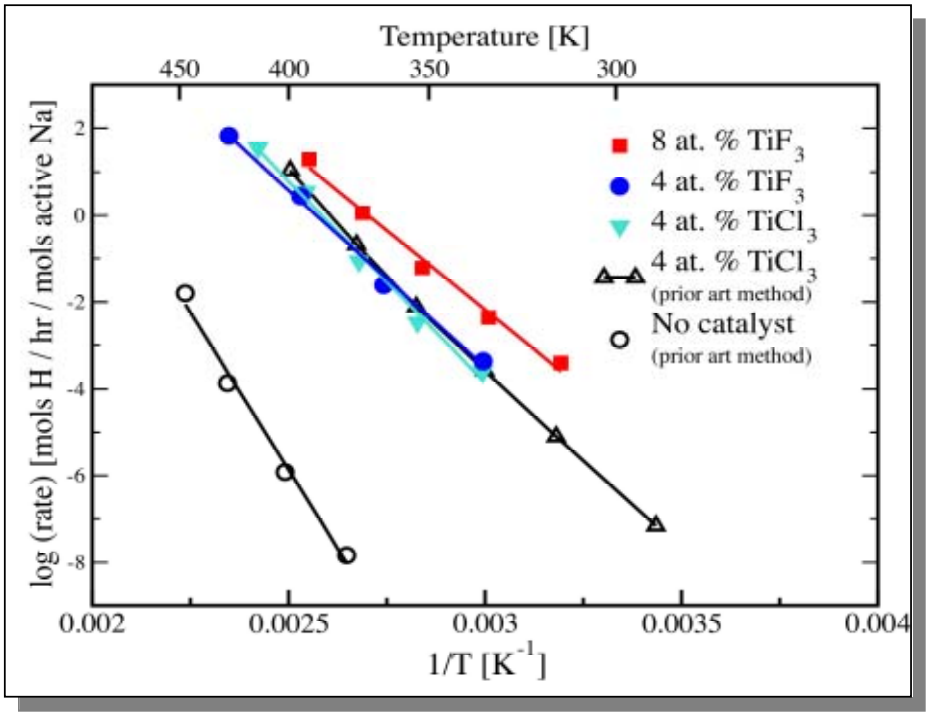

Figure 4 – Arrhenius plot of the hydrogen desorption rates vs. 1/T for the decomposition of $NaAlH_4$.

This particular sample shows poor kinetics as shown by the relatively long absorption (5 hours) and desorption (6 hours) times. We have tested different qualities of starting chemicals. It is clear that the quality of the starting materials used in the preparation process is critical for good hydrogen storage performance. These issues are currently being addressed at our facility.

Materials Compatibility Studies

Referring to equation 1, it should be noted that bulk metallic aluminum is formed as a product of the decomposition $NaAlH_4$ and of Na_3AlH_6 (Gross 1999). This metallic aluminum is consumed in the reverse hydride-formation reactions. We had concerns that the obvious choice for a hydride storage vessel, an aluminum pressure tank, might be a poor candidate for an alanate hydrogen-storage bed. The concern was that the integrity of an aluminum tank would be compromised by interaction with the alanate during cycling. To test this an initial experiment was performed using a 50% aluminum deficient mixture comprised of 2NaH + Al + 4 mol.% $TiCl_3$ (Majzoub 2001). A polished 6061 aluminum coupon was placed in intimate contact with this mixture and subjected to three hydrogen absorption / desorption cycles. The results are shown in figure 6. As

suspected, the coupon showed pitting where aluminum had been etched from the surface and consumed in the formation of the alanates.

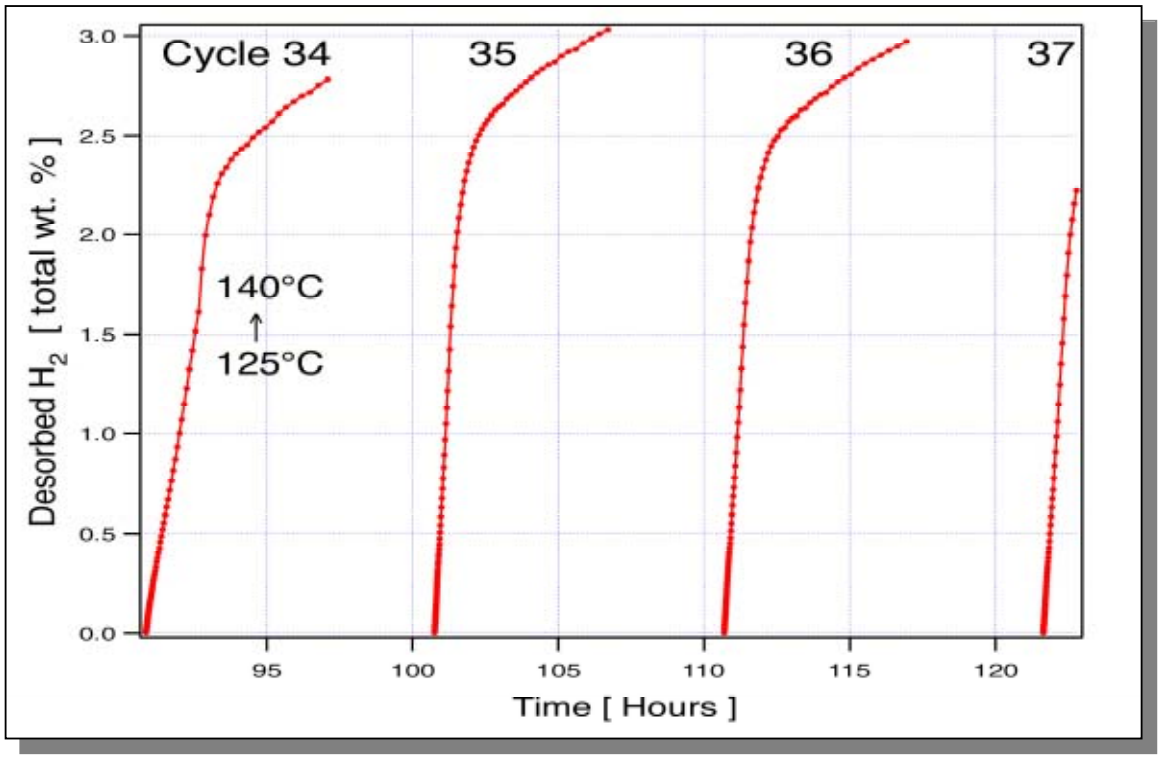

Figure 5 – Desorption Cycle-life measurements of 4 mol.% $TiCl_3$ doped $NaAlH_4$.

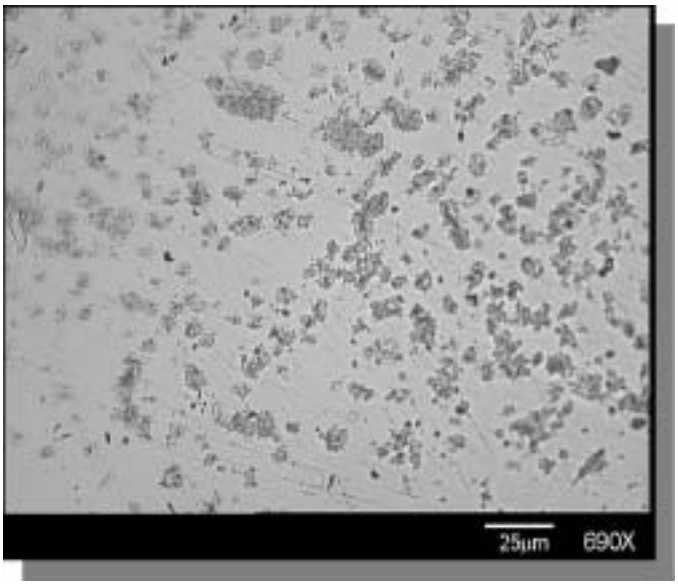

Figure 6 – Optical micrograph of a 6061 Al coupon exposed to an Al deficient sample of $NaAlH_4$ during three hydriding cycles.

These results lead us to perform more detail materials interaction test on three common containment vessel materials 6061 Al, 5083 Al, and 401L stainless steel. Tensile test specimens of these materials were subjected to controlled environments using an automated-apparatus for high-pressure hydrogen cycling (Figure 7). This was done under more realistic conditions designed to simulate use in typical hydrogen storage applications.

A)

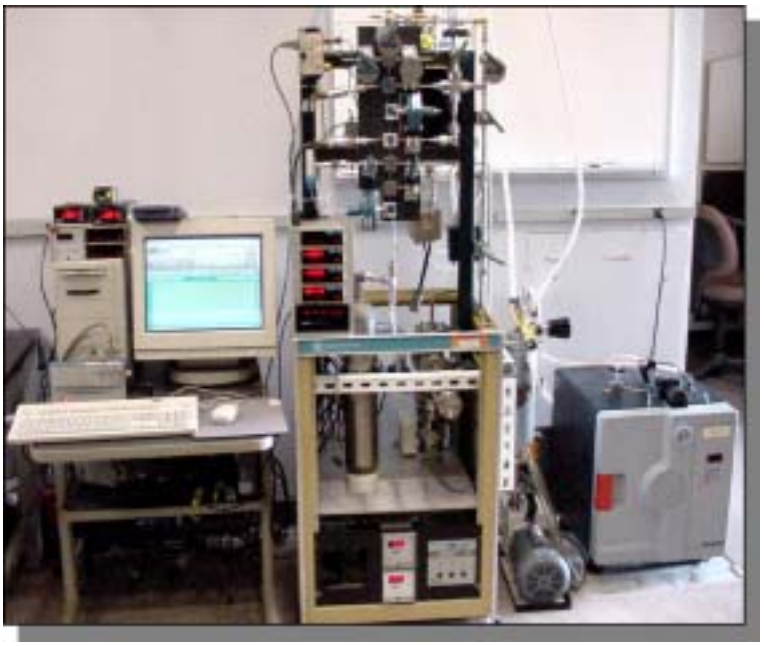

B)

Figure 7 – Tensile test coupons (A) and cycling apparatus (B)

Identical specimens of each material were simultaneously subjected to the following conditions at 125°C: 1) constant heating in an argon atmosphere, 2) 116 hydrogen absorption and desorption cycles without alanates, and 3) 116 hydrogen absorption and desorption cycles in intimate contact with 4 mol% $TiCl_3$ doped $NaAlH_4$. In this case, the alanate sample was not aluminum deficient. The hydrogen over-pressure during absorption varied between 140 and 80 bar. The pressure drop with each absorption cycle is shown in Figure 8. The two discontinuities indicate that the hydrogen gas bottle was changing out. The third absorption half-cycle is shown in red. Clearly, the alanates were still reversibly absorbing hydrogen on the 116th cycle.

Tensile testing of the specimens showed no degradation effects due to any interactions with the alanates. The only observable effect was hydrogen-induced degradation of the stainless steel samples independent of whether alanate was present or not (Majzoub 2001).

Scaled-up Test Bed Results

As a continuation of our engineering activities, we analyzed the results of measurements conducted on a scaled-up test bed. The bed was of a tubular design, 24.5 cm long stainless steel tube 3.17 cm diameter by 0.21 cm wall thickness (Figure 8). It was loaded with 72 g of 4 mol% $TiCl_3$ catalyzed $NaAlH_4$ (generation II) and evaluated over four complete discharge/charge

cycles. Thermocouples were placed at top, middle and bottom of thin-walled tubing running the length of the bed and along the outside of the bed. The internal thermocouple wells were placed in the center and at mid-radius in the bed (Figure 9). The instrumented reactor, wrapped with electrical heating tape, was evaluated on a new apparatus built for that purpose (Figure 8). It was designed for isobaric charging, followed by non-isobaric discharging into a large calibrated volume. All data was logged via computer for subsequent analysis. Charging runs were done at 125˚C at 60, 75 and 90 atm applied hydrogen pressure. For comparison purposes, an additional charging run was done at 100˚C and 90 atm. Discharging runs were performed at 80, 100, 125 and 150˚C.

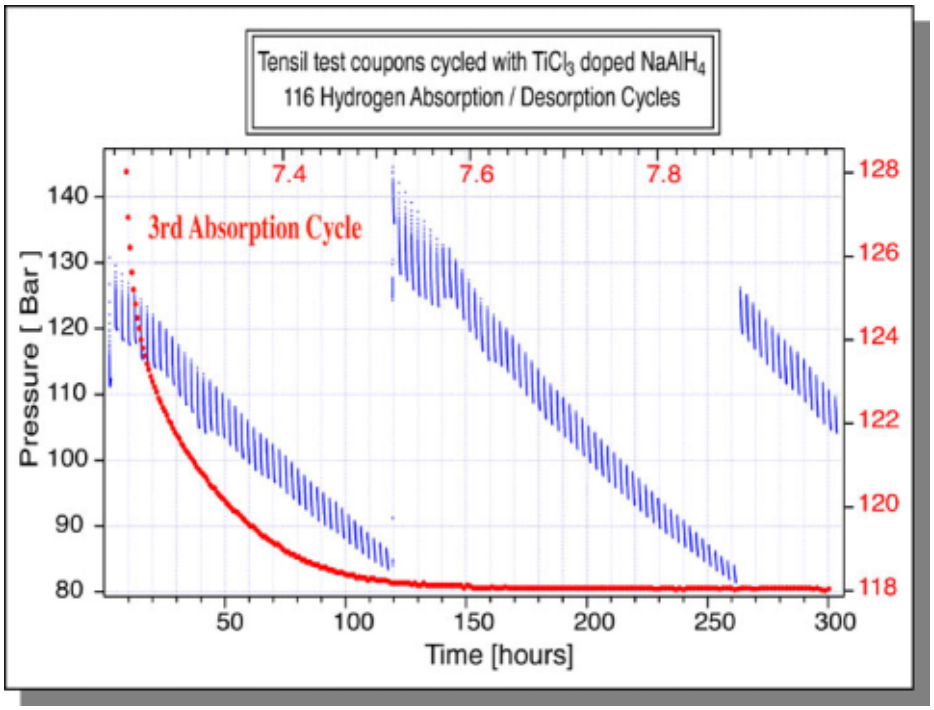

Figure 8 – Applied hydrogen pressure during 116 absorption/desorption cycles.

The reversible capacity of 3.4 total wt.% H_2 was low, but expected because of the inherent losses that result from the Generation II catalyzing reaction (reaction of the $TiCl_3$ catalyst precursor with some of the $NaAlH_4$ to form NaCl). Hydrogen absorption is quite rapid for the formation of Na_3AlH_6. The bend in the absorption curve (Figure 10) indicates completion of this reaction. $NaAlH_4$ forms more slowly.

The internal thermocouple trace temperatures showed very little difference for both absorption and desorption. These are shown as the red and black traces in Figure 10 and Figure 11. This small temperature gradient indicates a low coefficient of thermal conductivity K_{th}. The exothermic nature of the absorption reaction causes the temperature to rapidly increase in the bed upon hydriding. However, the peak temperature remains below Na_3AlH_6 plateau temperature at the applied pressure. On the other hand, the temperature is above the plateau temperature for $NaAlH_4$ and so this phase does not begin to form until the temperature drops below about 160°C. At this temperature, there is a slight change in the slope of the temperature profiles and hydrogen absorption begins to pickup again as the higher capacity phase begins to

form. A very small amount of $NaAlH_4$ may have formed in the initial moments before the temperature exceeded the plateau temperature of this phase. $NaAlH_4$ melts at 180°C so any of this phase that was present was melted in the initial part of the hydrogen loading. This would explain the observed sintering of the material into a rigid but porous mass. Prior experiments showed that this sintering was not detrimental to hydrogen absorption or desorption. In fact, it may be an added advantage when compared to classic metal hydrides which have problems associated with migration of fine powders and packing.

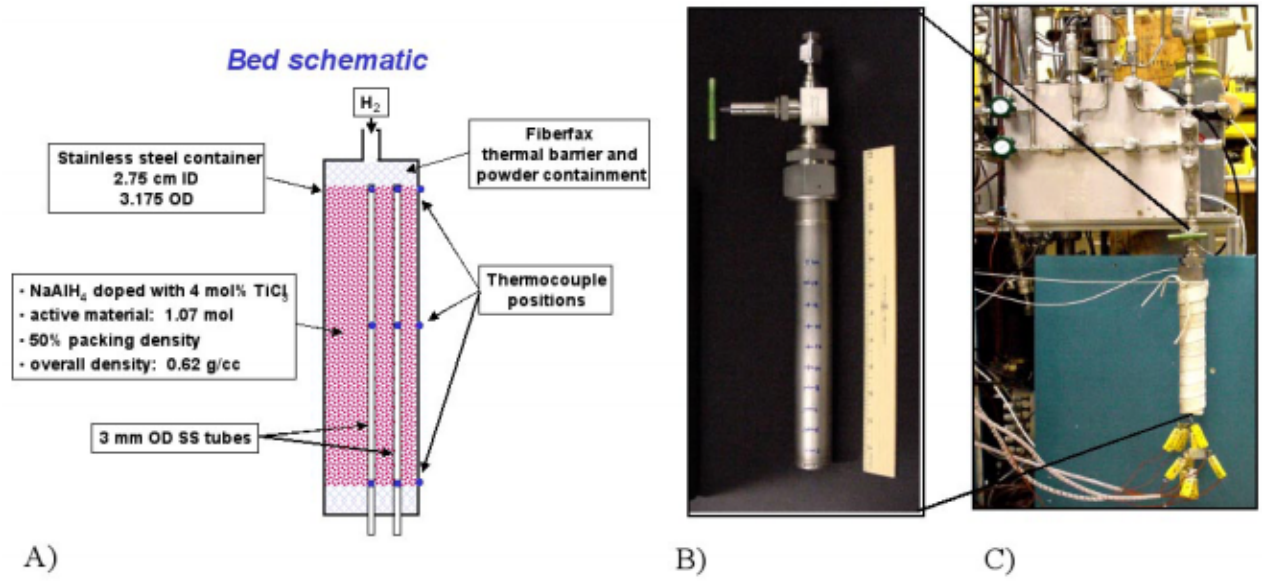

Figure 9 – Scaled-up Bed and test stand showing control manifold, tape heater and axial thermocouples.

For the desorption measurements the reactions are endothermic and so there is a characteristic drop in the bed temperature (Figure 11). This reduction in temperature slows the desorption rate. Desorption is the opposite of absorption in that the decomposition of $NaAlH_4$ is much faster that that of Na_3AlH_6. The $NaAlH_4$ is nearly fully decomposed after 1 hour. Finally, the small temperature between the internal thermocouples is consistent with absorption results, which suggests low thermal conductivity.

The thermal properties of the bed were modeled using a solution for an infinite cylinder geometry (Carslaw and Jaeger). The effective thermal conductivity (K_{th}) in the present bed is slightly lower, but typical of intermetallic hydride beds:

K_{th} (alanate) = 4-5 X 10-4 cal/(sec-cm-K) = ~2 X 10-3 joule/(sec-cm-K) = 0.2 watt/(m-K)

K_{th} (IM hydride) = 0.4 watt/(m-K)

As with intermetallic hydrides, the inter-particle thermal resistance is very high. This demonstrates the need for internal structures designed for thermal control.

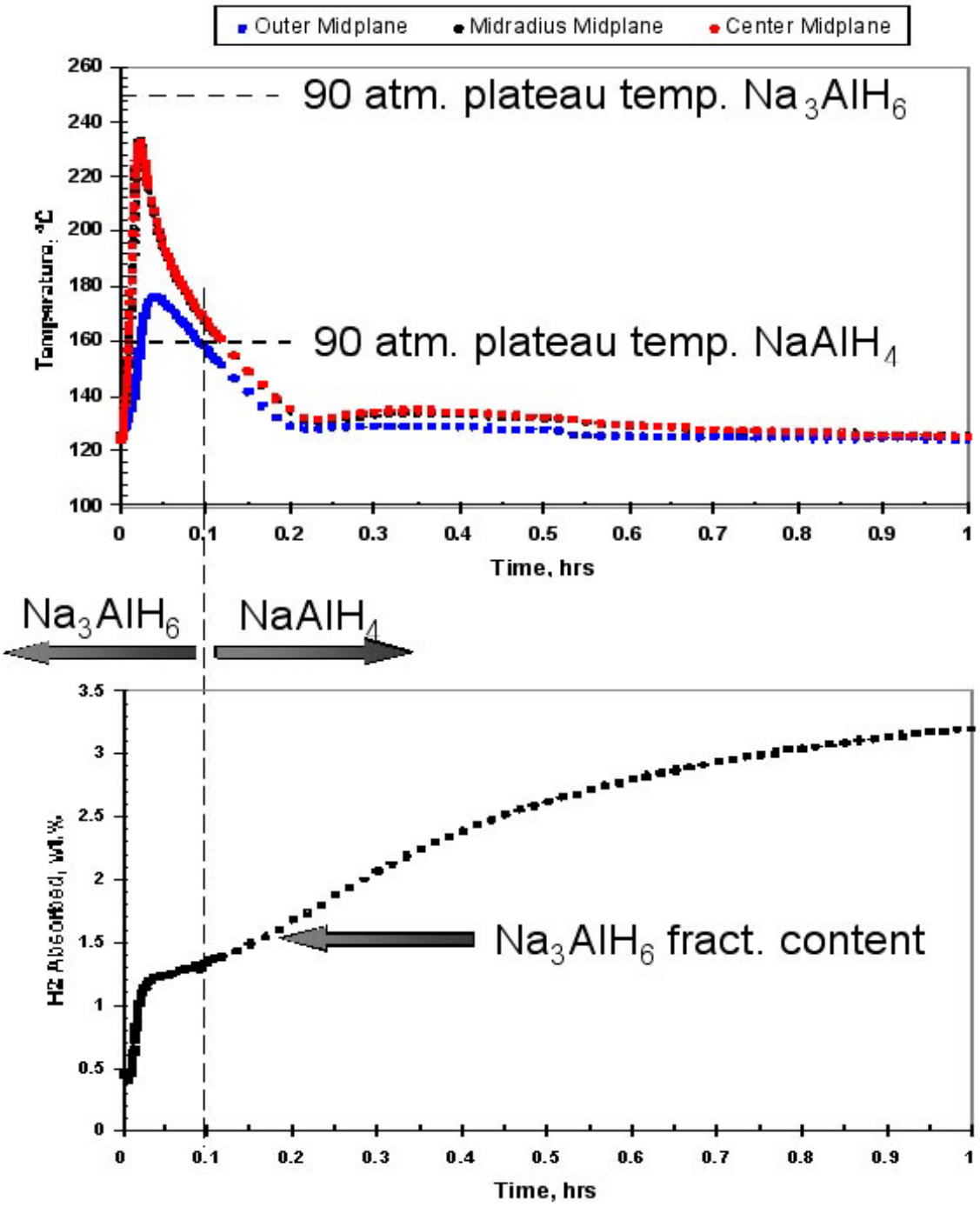

Figure 10 – Third hydrogen absorption of the scaled-up test bed.
(Top: temperature profiles, Bottom: volumetrically measured hydrogen absorbed)

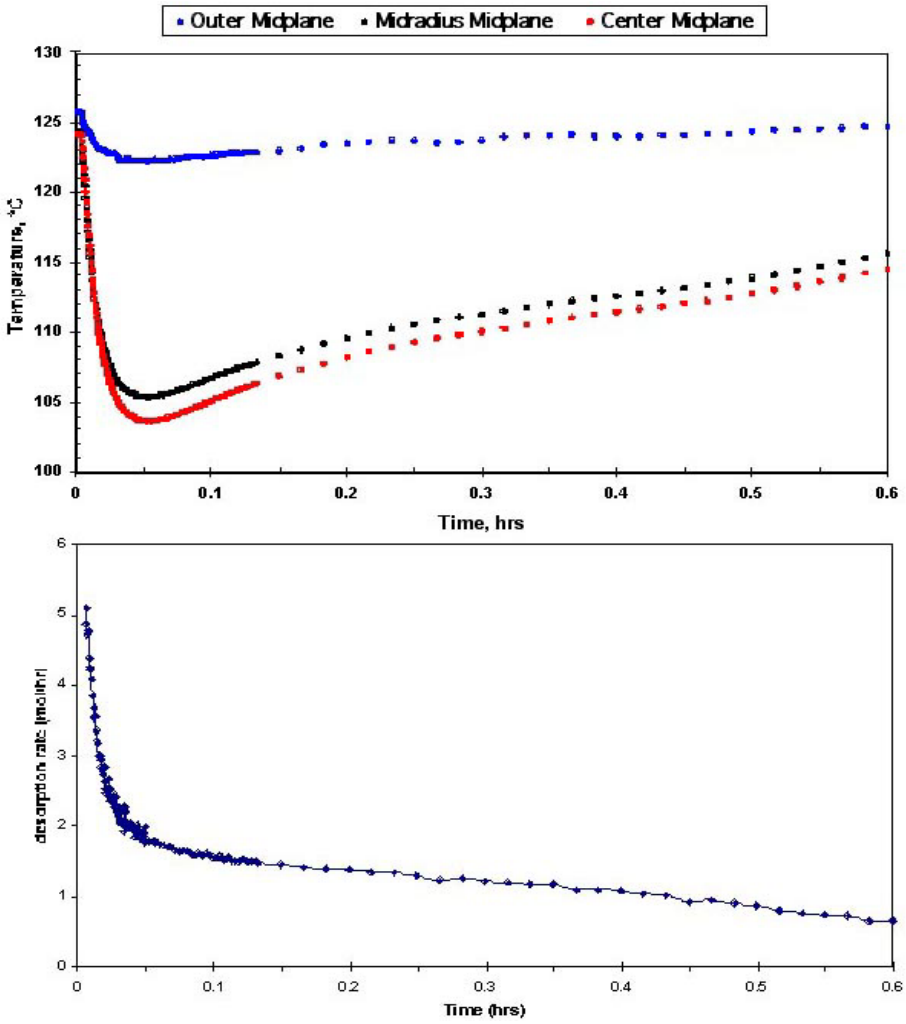

Figure 11 – Third hydrogen desorption of the scaled-up test bed.
(Top: temperature profiles, Bottom: volumetrically measured hydrogen desorbed)

Conclusion

The advances that have been achieved this year include:

1) The development of a synthesis route to produce Na_3AlH_6 and $NaAlH_4$ directly from Na and Al metals (Patent application submitted).
2) The discovery that it is the Titanium that contributes to the enhanced kinetics, the Ti-halide precursor gives the same results independent of the halide that is used.
3) For that reason, the use of Ti-fluorides or lower Cl content chlorides will provide an incremental improvement in the reversible weight capacity.
4) A preliminary investigation shows that the direct synthesized alanates undergo an activation consisting of 2-3 cycles. Following this, it appears that the capacity and rates are quite stable after many cycles.

5) Aluminum is consumed in forming the alanates. It was found that it doesn't matter where the aluminum comes from (i.e. Sorption materials or container vessel walls). However, the use of alanates that are not aluminum deficient, did not appear to degrade the strength of aluminum-based alloys in when tested under long-term cycling conditions.

6) Scaled-up bed studies demonstrated the large and somewhat complex thermal effects that can occur during hydrogen absorption and desorption from scaled-up quantities of the alanates. While some sintering occurs, the thermal conductivity of the alanate matrix is very nearly the same as that of hydrides in a packed-powder bed.

In summary, these results demonstrate that solid progress is being made on the development of alanates for mobile hydrogen storage applications.

Future work

Our future work is now focused on further improving the capacity and kinetics of the latest generation of alanates. These materials will be examined through extensive cycle-life and scale-up studies. We are also expanding the new synthesis and catalyst doping technique to other novel complex hydrides. Finally, we will focus on gaining a better understanding of the mechanism by which Ti-doping enhances the kinetics of these gas/solid-state reactions.

Acknowledgements

We thank Scott Spangler, Andres Orozco, and Don Meeker of SNL for their expert help in all aspects of the materials preparation and experimental measurements and Ken Stewart of SNL for all of his contributions in developing our experimental equipment.

References

Bogdanovic', B. and Schwickardi, M. 1997. "Ti-doped alkali metal aluminum hydrides as potential novel reversible hydrogen storage materials", *J. Alloys and Compounds*, **253**:1.

Bogdanovic', B., Brand, R.A., Marjanovic', A., Schwikardi, M., and Tölle, J. 2000. "Metal-doped sodium aluminum hydrides as potential new hydrogen storage materials", *J. Alloys and Compounds*, **302**:36.

Bogdanovic B., Schwickardi M. 2001. "Ti-doped $NaAlH_4$ as a hydrogen-storage material – preparation by Ti-catalyzed hydrogenation of aluminum powder in conjunction with sodium hydride", *Applied Physics A*, 72 (#2):221.

Gross, K.J., Guthrie, S.E., Takara, S., and Thomas, G.J. 1999. "*In situ* X-ray diffraction study of the decomposition of $NaAlH_4$", *J. Alloys and Compounds*, **297**:270.

Gross, K.J., Thomas, G.J., and Sandrock, G., 2000. "Hydride development for hydrogen storage", in *Proceedings U.S. DOE Hydrogen Program Review*, NREL/CP-570-26938,452. Baltimore, MD.

Gross, K.J., Thomas, G.J., and Jensen, C.M., 2001a. "Catalyzed Alanates for Hydrogen Storage", In *Proceedings of the International Symposium on Metal Hydrogen Systems*, Noosa, Australia, Oct. 2000.

Gross, K. J., Thomas, G. J., Majzoub, E. and Sandrock, G. 2001b "Light-weight Hydride Development" ", in *Proceedings U.S. DOE Hydrogen Program Review*, NREL/CP-570-30535 San Ramon, CA

Jensen, C.M., Zidan, R.A., Mariels, N., Hee, A.G., and Hagen, C. 1999. "Advanced titanium doping of sodium aluminum hydride: segue to a practical hydrogen storage material?", *Int. J. Hydrogen Energy*, **24**:461.

Jensen C.M., Gross K.J. 2001. "Development of Catalytically Enhanced Sodium Aluminum Hydride as Hydrogen Storage Material", *Applied Physics A*, 72(#2):221.

Majzoub, E.H., Somerday, B.P., Goods, S.H., and Gross, K.J. 2001. "Interaction between sodium aluminum hydride and candidate containment materials", *Proceedings of the conference on Hydrogen Effects on Material Behavior*, Jackson Hole Wyoming, N. Moody editor.

Sandrock, G., Gross, K., Thomas, G., Jensen, C., Meeker, D. and Takara, S. 2001. "Engineering considerations in the use of catalyzed sodium alanates for hydrogen storage" In *Proceedings of the International Symposium on Metal Hydrogen Systems*, Noosa, Australia, Oct. 2000.

Sandrock, G., Gross, K., Thomas, G. 2002. "Effect of Ti-catalyst content on the reversible hydrogen storage properties of the sodium alanates", *J. Alloys and Compounds* **339**:299.

Thomas, G.J., Guthrie, S.E., and Gross, K. 1999. "Hydride development for hydrogen storage", in *Proceedings U.S. DOE Hydrogen Program Review*, NREL/CP-570-26938,452. Denver CO.

Zaluska, A., Zaluski, L., and Ström-Olsen, J.O. 2000. "Sodium alanates for reversible hydrogen storage", *J. Alloys and Compounds*, **298**:125.

Zaluska A., Zaluski L., Strom-Olsen J.O. 2001. "Structure, catalysis and atomic reactions on the nano-scale: a systematic approach to metal hydrides for hydrogen storage", *Applied Physics A*, 72(#2):157.

Zidan, R.A., Takara, S., Hee, A.G., and Jensen, C.M. 1999. "Hydrogen Cycling Behavior of Zirconium and Titanium-Zirconium Doped Sodium aluminum Hydride", *J. Alloys and Compounds*, **285**:119.